Riv. Mat. Univ. Parma (4) **16** (1990), 47-61

DIEGO ROCCATO and EPIFANIO VIRGA (*)

Drops of nematic liquid crystals floating on a liquid (**)

A TRISTANO MANACORDA per il suo 70° compleanno

1 - Introduction

In Kléman's book [4] there is a picture, apparently shot by P. Piéranski, which shows drops of nematic liquid crystals floating on gelatine (cf. plate III of p. XVI). We were fascinated by the shape of those drops. They appeared to us as balls bearing a crater underneath the plane of buoyancy. It is the purpose of this paper to explain such a shape.

The main outcomes of the work presented here have been shortly reported without proof in a paper by Virga [10]. We refer to Section 5 of [10] for a detailed mathematical setting of the problem and the class of shapes within which we look for minimizers of the free energy.

The plan of the paper is as follows. In **1** we specify the bulk free energy and the surface tension of the floating drops. For the former we adopt Frank's formula (see [2]). For the latter we adopt Rapini-Papoular's formula (see [1] and also [9]) expressed in terms of a dimensionless parameter ω, which, for a given substrate, is a function of the temperature. In **2** we lay assumptions that simplify the variational problem and permit us to solve in **3** the equilibrium equations. The stable shapes of the drops correspond to the solutions of the equilibrium equations that minimize the free energy. In **4** we determine the stable shapes of the drops for all values of ω and we find a bifurcation with exchange of stability at $\omega = 1$. In **5** we explore some features of the stable shapes corresponding to very

(*) Indirizzo: Dipartimento di Matematica, Università, I-27100 Pavia.
(**) Ricevuto: 1-II-1990.

large values of ω. Although these shapes are unlikely to be observed, we have paid attention to them to check the consistency of our analysis.

1 - Energy functional

Let $\mathscr{B}$ be the region of space occupied by a drop of nematic liquid crystal. The orientation of the optical axis in the liquid crystal is described by the unit vector $\boldsymbol{n}$. According to the theory of Oseen [7] and Frank [2], the bulk free energy of the drop is the functional

$$\mathscr{F}_{\text{bulk}}[\mathscr{B}, \boldsymbol{n}] = \int_{\mathscr{B}} \sigma(\boldsymbol{n}, \nabla \boldsymbol{n}) \tag{1.1}$$

where the function σ is given by the classical formula (see [2])

$$\sigma(\boldsymbol{n}, \nabla \boldsymbol{n}) = k_1(\operatorname{div} \boldsymbol{n})^2 + k_2(\boldsymbol{n} \cdot \operatorname{curl} \boldsymbol{n})^2 + k_3|\boldsymbol{n} \wedge \operatorname{curl} \boldsymbol{n}|^2 + (k_2 + k_4)(\operatorname{tr}(\nabla \boldsymbol{n})^2 - (\operatorname{div} \boldsymbol{n})^2). \tag{1.2}$$

In (2) the coefficients k_1, k_2, k_3 and k_4 are material moduli depending on the temperature (which is taken as constant throughout this paper).

When the drop that occupies $\mathscr{B}$ is in contact with an isotropic fluid, the free energy of the interface between the two fluids is the functional

$$\mathscr{F}_{\text{interface}}[\mathscr{S}, \boldsymbol{n}] = \int_{\mathscr{S}} w(\boldsymbol{n} \cdot \boldsymbol{\nu}) \tag{1.3}$$

where $\mathscr{S}$ is the surface of contact and $\boldsymbol{\nu}$ is the outer unit normal to $\mathscr{B}$. It is customary to call ϑ the angle between $\boldsymbol{n}$ and $\boldsymbol{\nu}$, often referred to as the *tilt angle*, and to employ the following formula for w (see e.g. [9])

$$w(\cos \vartheta) = w_0 + w_1 \cos^2 \vartheta + w_2 \cos^4 \vartheta \tag{1.4}$$

where w_0, w_1 and w_2 are material moduli depending on both the temperature and the nature of the fluids in contact. For simplicity in this paper we set $w_2 = 0$ and $w_1 = \omega w_0$. Thus (4) reduces to

$$w(\cos \vartheta) = w_0(1 + \omega \cos^2 \vartheta) \tag{1.5}$$

with $w_0 > 0$ and $\omega > -1$. This is the well-known formula of Rapini and Papoular that has been recently confirmed by some experiments (cf. e.g. [6] and [8]).

The drop we consider in this paper is in contact with two isotropic fluids: namely, a liquid and a gas above it. We denote by $\mathcal{S}^+$ and $\mathcal{S}^-$, respectively, the *emerging boundary* and the *submerged boundary* of the drop. The former is the interface between the liquid crystal and the gas while the latter is the interface between the liquid crystal and the liquid. Thus the total free energy of the drop is given by

$$\mathcal{F}[\mathcal{B}, \boldsymbol{n}] = \mathcal{F}_{\text{bulk}}[\mathcal{B}, \boldsymbol{n}] + \mathcal{F}_{\text{surface}}[\mathcal{B}, \vartheta] \qquad \text{where} \tag{1.6}$$

$$\mathcal{F}_{\text{surface}}[\mathcal{B}, \vartheta] = \int_{\mathcal{S}^+} w_0^+(1 + \omega^+ \cos^2\vartheta) + \int_{\mathcal{S}^-} w_0^-(1 + \omega^- \cos^2\vartheta). \tag{1.7}$$

The moduli w_0^+, ω^+ and w_0^-, ω^- pertain, respectively, to the emerging and submerged boundaries of the drop. When a pair $(\mathcal{B}, \boldsymbol{n})$ minimizes $\mathcal{F}$, we briefly say that $\mathcal{B}$ is a *stable shape* and that $\boldsymbol{n}$ is a *stable orientation.*

For the problem we are concerned with, liquid crystals can be taken as incompressible fluids. Hence the volume of the drop is prescribed. A further constraint comes from the law of buoyancy, which prescribes the volume of the submerged part.

In the scheme described so far, the problem of finding both the stable shape and the stable orientation is still too hard to solve. We put aside the purpose of finding the stable orientation and we confine ourselves to seek the shape, once the orientation has been somehow prescribed.

Furthermore, as pointed out in Sect. 3 of [10], for many liquid crystals the surface free energy prevails over the bulk free energy. In fact, $\mathcal{F}_{\text{surface}} \sim \bar{w}R^2$ and $\mathcal{F}_{\text{bulk}} \sim \bar{k}R$, where R is the linear dimension of the drop and $\bar{w}$, $\bar{k}$ are, respectively, the order of magnitude of the surface and bulk material moduli. Hence

$$\frac{\mathcal{F}_{\text{surface}}}{\mathcal{F}_{\text{bulk}}} \gg 1 \quad \text{if} \quad R \ll \frac{\bar{k}}{\bar{w}}.$$

The latter inequality is often verified: for MBBA at room temperature, for example, $\bar{k}/\bar{w} \sim 10^{-8}$ cm (cf. [3] and [5]). *Thus from now on we neglect* $\mathcal{F}_{\text{bulk}}$ *in the total free energy.*

In 2 we set up the preliminaries that enable us to find approximate stable shapes of the drop.

2 - Variational problem

For many nematic liquid crystals there is much evidence (cf. [4], p. 57) that the homeotropic anchoring condition holds at the emerging boundary of the drop whenever the gas is air: $\vartheta = 0$ on $\mathcal{S}^+$. If the volume of the submerged part is much smaller than the total volume, one expects the emerging boundary to be spherical and the stable orientation to be the radial field $\boldsymbol{n} = \boldsymbol{e}_r$, often referred to as a *hedgehog*. We call $\mathcal{B}_0$ the ball whose boundary contains $\mathcal{S}^+$ and whose center is the singular point of $\boldsymbol{n}$.

The problem of minimizing the total free energy of the drop reduces to: *Find the surface* $\mathcal{S}^-$ *that minimizes*

$$\mathcal{F}_{\text{interface}}[\mathcal{S}^-, \vartheta] = \int_{\mathcal{S}^-} w_0^-(1 + \omega^- \cos^2\vartheta) \tag{2.1}$$

subject to

$$\text{vol}(\mathcal{B}) = \beta \qquad \beta > 0 \tag{2.2}$$

$$\text{vol}(\mathcal{B}^-) = \beta^- \qquad \beta^- > 0 \tag{2.3}$$

where vol *denotes the volume measure and* $\mathcal{B}^-$ *is the submerged part of* $\mathcal{B}$.

We now describe the special class of surfaces $\mathcal{S}^-$ in which we look for a solution of this problem. We take $\mathcal{S}^-$ to be symmetric about $\boldsymbol{e}_z$, the vertical axis passing through the center of $\mathcal{B}_0$. We assume that the intersection of $\mathcal{S}^-$ and any plane containing $\boldsymbol{e}_z$ is represented by a function $\rho(\varphi)$. The co-ordinates (ρ, φ) are illustrated in Figure 1, which represents a section of the drop.

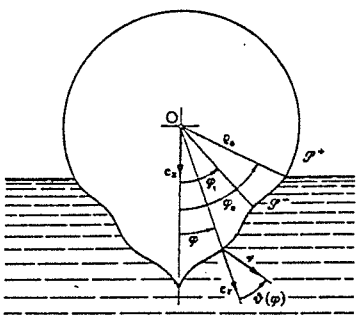

Fig. 1.

Now both ρ_0, the radius of $\mathscr{B}_0$, and φ_0, the angle where $\mathcal{S}^-$ and $\mathcal{S}^+$ touch each other, are regarded as prescribed. They are to be used later to fulfill the constaints (2) and (3). The function $\rho(\varphi)$ can easily be expressed in terms of the tilt angle ϑ

$$\rho(\varphi) = \rho_0 \exp[-\int_{\varphi_0}^{\varphi} \operatorname{tg} \vartheta(\xi)\, d\xi]. \tag{2.4}$$

As shown in Fig. 1, we take the surface $\mathcal{S}^-$ to be spherical for $\varphi_0 \leqslant \varphi \leqslant \varphi_1$. In other words, $\vartheta(\varphi)$ is equal to 0 for $\varphi_0 \leqslant \varphi \leqslant \varphi_1$ and it is a function of class C^1 for $0 \leqslant \varphi < \varphi_1$. Such a choice should not be restrictive whenever the surface moduli w_0^+ and w_0^- do not differ too much. Note that $\vartheta(\varphi)$ need not be continuous: it may suffer a jump at $\varphi = \varphi_1$. So doing we allow $\mathcal{S}^-$ to possess an edge, thoug we do not account for any energy distribution along it. If $\varphi_1 = 0$ then $\vartheta \equiv 0$ and the corresponding surface $\mathcal{S}^-$ is part of a sphere. If $\varphi_1 > 0$ and $\vartheta(\varphi) > 0$, $\mathcal{S}^-$ represent a *bump* outside $\mathscr{B}_0$; if, on the contrary, $\vartheta(\varphi) < 0$, $\mathcal{S}^-$ represents a *crater* inside $\mathscr{B}_0$.

We employ the change of variables

$$\phi(\varphi) = \int_{\varphi_1}^{\varphi} tg\, \vartheta(\xi)\, d\xi. \tag{2.5}$$

By (5), (4) can be rewritten as

$$\rho(\varphi) = \begin{cases} \rho_0 e^{-\phi(\varphi)} & \text{for } 0 \leqslant \varphi \leqslant \varphi_1 \\ \rho_0 & \text{for } \varphi_1 \leqslant \varphi \leqslant \varphi_0. \end{cases} \tag{2.6}$$

By use of (6), (1) becomes a functional of ϕ that depends on φ_1

$$\mathscr{F}[\varphi_1, \phi] = 2\pi\rho_0^2 w_0 \Big(\int_0^{\varphi_1} e^{-2\phi(\varphi)} \frac{1 + \omega + (\phi'(\varphi))^2}{[1 + (\phi'(\varphi))^2]^{1/2}} \sin\varphi\, d\varphi \tag{2.7}$$

$$+ (1 + \omega)(\cos\varphi_1 - \cos\varphi_0) \Big)$$

where we have replaced w_0^- and ω^- by w_0 and ω, respectively, to avoid clutter.

The admissible shapes of the drop are described by the pairs (φ_1, ϕ). An equilibrium shape corresponds to a pair that makes $\mathscr{F}$ stationary. A stable shape corresponds to a pair that minimizes $\mathscr{F}$. Thus our variational problem is: *Find* $\varphi_1 \in [0, \varphi_0]$ *and* ϕ *of class* $C^2(0, \varphi_1)$ *that minimizes* $\mathscr{F}$ *subject to*

$$\phi(\varphi_1) = 0. \tag{2.8}$$

In 3 we go through the mathematical analysis that is needed to open the way to the numerical solution of this problem.

3 - Equilibrium equations

If the pair (φ_1, ϕ) represents an equilibrium shape of the drop, then $\mathscr{F}[\varphi_1, \phi]$ is stationary with respect to the variations of both φ_1 and ϕ. By computing these variations we are led to the equilibrium equations of $\mathscr{F}$:

$$\frac{1+\omega+(\phi'(\varphi_1))^2}{[1+(\phi'(\varphi_1))^2]^{1/2}}-(1+\omega)=0 \tag{3.1}$$

$$\lim_{\varphi\to 0^+}(e^{-2\phi(\varphi)}\frac{1-\omega+(\phi'(\varphi))^2}{[1+(\phi'(\varphi))^2]^{3/2}}\phi'(\varphi)\sin\varphi)=0 \tag{3.2}$$

$$\frac{\mathrm{d}}{\mathrm{d}\varphi}(e^{-2\phi(\varphi)}\frac{1-\omega+(\phi'(\varphi))^2}{[1+(\phi'(\varphi))^2]^{3/2}}\phi'(\varphi)\sin\varphi) \tag{3.3}$$

$$+2e^{-2\phi(\varphi)}\frac{1+\omega+(\phi'(\varphi))^2}{[1+(\phi'(\varphi))^2]^{1/2}}\sin\varphi=0 \qquad \text{in }]0,\ \varphi_1[\,.$$

Equation (1), which results from the variation of φ_1, constrains the value of $\phi'(\varphi_1)$; equation (2) is the natural boundary condition for ϕ' at $\varphi=0$. For ϕ of class C^2 both ϕ and ϕ' are bounded near 0, and so equation (2) is always satisfied. By use of the change of variables

$$\tau=\operatorname{tg}\varphi \qquad t=\operatorname{tg}\vartheta=\phi' \tag{3.4}$$

equations (1) and (3) become, respectively,

$$\frac{1+\omega+t^2(\tau_1)}{1+t^2(\tau_1))^{1/2}}-(1+\omega)=0 \tag{3.5}$$

$$t'=-\frac{1+t^2}{1+\tau^2}\,\frac{2\tau(1+\omega+(2\omega+1)t^2)+t(1-\omega+t^2)}{\tau(1-\omega+(2\omega+1)t^2)} \qquad \text{in }]0,\ \tau_1[\tag{3.6}$$

where $\tau_1=\operatorname{tg}\varphi_1$ and the function $t:[0,\ \tau_1]\to\mathbb{R}$ is of class C^1.

Let h be the function defined by

$$h(t)=\frac{1+\omega+t^2}{(1+t^2)^{1/2}}-(1+\omega). \tag{3.7}$$

The graph of h is plotted in Figure 2. When $-1<\omega\leqslant 1$, h vanishes only at 0. When $\omega>1$, h vanishes at $-\hat{t}$, 0, $\hat{t}$ and it is minimum at $-t_0$ and t_0, being

$$\hat{t}=(\omega^2-1)^{1/2} \qquad t_0=(\omega-1)^{1/2}. \tag{3.8}$$

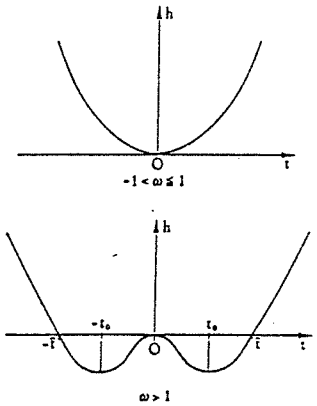

Fig. 2.

Thus $t(\tau_1)$ is uniquely determined when $-1<\omega\leqslant 1$, while it may take three different values when $\omega>1$. The role played by t_0 will be clear in the following.

Now, for every $\omega>-1$, we seek $\tau_1\geqslant 0$ and a solution of (6) such that $t(\tau_1)$ be prescribed according to (5). Of course, $\tau_1=0$ and $t(\tau_1)=0$ represent a trivial solution in the class we employ. The shape of the drop corresponding to such a solution is the ball $\mathscr{B}_0$.

If $-1<\omega<-\frac{1}{2}$, the half-plane $\mathscr{H}=\{(\tau,\ t)\in\mathbb{R}^2|\tau\geqslant 0\}$ splits into several regions in each of which the sign of t' is constant, as Figure 3 illustrates for $\omega=-0.75$.

Along the lines of $\mathscr{H}$ defined by the equations $\tau=0$, $t=\bar{t}$, and $t=-\bar{t}$, where

$$\bar{t}=\left(\frac{\omega-1}{2\omega+1}\right)^{1/2} \tag{3.9}$$

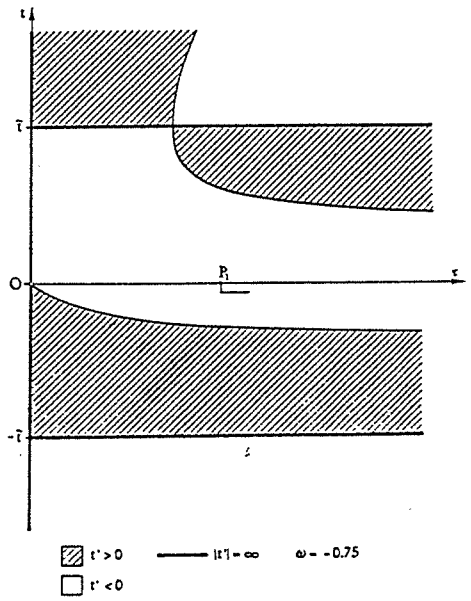

Fig. 3.

t' becomes unbounded. It is easily seen that the graph of any solution of (6) can touch the axis $\tau = 0$ only at the origin. A close inspection of Fig. 3 shows that no solution of (6) passing through any point $P_1 = (\tau_1, 0)$ can be continued up to $\tau = 0$, unless $\tau_1 = 0$. *Thus the ball $\mathscr{B}_0$ is the only equilibrium shape of the drop in the class we employ.*

If $-\frac{1}{2} \leqslant \omega \leqslant 1$, there is only one region of $\mathscr{R}$ where t' is positive and only one where it is negative, as is shown in Figure 4 for $\omega = -0.2$. The analysis above

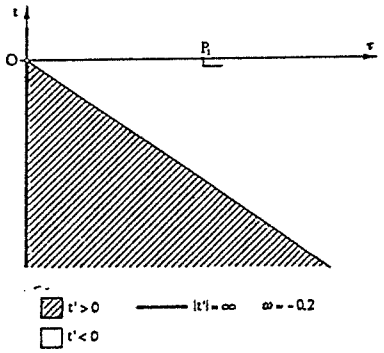

Fig. 4.

still applies, but a new case arises: the solution of (6) passing through a point P_1 might approach $t=\infty$ as $\tau\to 0$. That this case does not occur follows easily from the approximate form of (6) when $t\approx\infty$

$$t' = -\frac{1}{2\omega+1}\frac{t^3}{\tau}. \tag{3.10}$$

The solution of (10) is indeed

$$t(\tau) = \left(\frac{2\omega+1}{\log\tau + c}\right)^{1/2} \tag{3.11}$$

where c is a constant, and so $t(\tau)$ may approach ∞ only when τ approaches a *positive* number. Once again all solutions of (6) passing through any P_1 cannot be continued up to $\tau=0$, and $\mathscr{B}_0$ *is the only equilibrium shape of the drop.*

If $\omega>1$, the analysis of (6) is more complex. Figure 5 illustrates the regions of $\mathscr{H}$ where the sign of t' is constant when $\omega=5$. The solution of (6) can touch the axis $\tau=0$ either at $t=0$ or at $t=\pm t_0$ (cf. $(8)_2$). The points P_1, P_1', and P_1'' correspond to the three admissible values of $t(\tau_1)$. By repeating the same

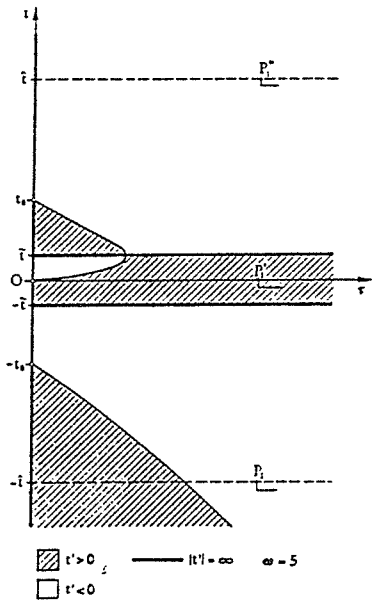

Fig. 5.

arguments as above we show that no solution of (6) passing through either any P_1' or any P_1'' can be continued up to $\tau = 0$. It remains to consider the solutions of (6) intersecting the line $t = -\hat{t}$. *Only one of these solutions can be continued up to* $\tau = 0$, i.e. *that reaching the point* $(0, -t_0)$. Thus we integrate (6) numerically starting from this point and call $\hat{P}_1$ the intersection between the graph of such a solution and the line $t = -\hat{t}$. The first co-ordinate of $\hat{P}_1$, $\hat{\tau}_1 = \operatorname{tg} \hat{\varphi}_1$, gives the only value of τ_1 that makes $\mathscr{T}$ stationary. The corresponding solution of (6) represents an *equilibrium shape* $\hat{\mathscr{B}}$ *that bears a crater underneath the plane of buoyancy.* We checked the accuracy of the calculation by halving the integration step.

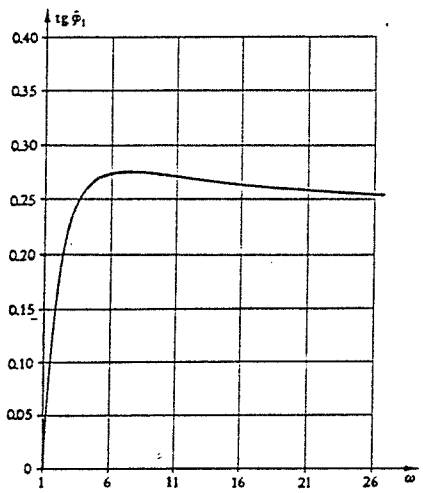

Fig. 6.

Figure 6 shows the graph of $\operatorname{tg} \hat{\varphi}_1$ as a function of ω. We will prove in 5 that the line $\operatorname{tg} \hat{\varphi}_1 = \frac{1}{4}$ is indeed an asymptote to the graph of Fig. 6. This will provide a further, independent check of the computation.

We conclude that when $-1 < \omega \leqslant 1$ the only equilibrium shape of the drop is the ball $\mathscr{B}_0$, with $\varphi_0 > 0$ and $\rho_0 > 0$ chosen so as to satisfy (2.2) and (2.3). When $\omega > 1$ there are two equilibrium shapes of the drop, namely $\mathscr{B}_0$ and $\hat{\mathscr{B}}$. By $(4)_2$, the latter can be represented through a function $\hat{\vartheta}$. It follows from $(8)_2$ that $\hat{\vartheta}$ satisfies

$$\hat{\vartheta}(0) = -\operatorname{arctg}(\omega - 1)^{1/2}. \tag{3.12}$$

It is understood that φ_0 and ρ_0 are chosen so as to satisfy (2.2) and (2.3).

$\hat{\mathcal{B}}$ possesses a sharp edge; it can be regarded as a close approximation of the smooth shape one expects when appropriate distributions of energy arise along the edges.

4 - Stable shapes

We see from Fig. 6 that $\hat{\varphi}_1$ approaches 0 as ω approaches 1. Thus $\mathcal{B}_0$ and $\hat{\mathcal{B}}$ represent, in a sense, the branches of a bifurcation occurring at $\omega = 1$. To figure out which of the two shapes is stable, we estimate the energy of both. We denote by $\mathcal{F}_0$ and $\hat{\mathcal{F}}$ the energy of $\mathcal{B}_0$ and $\hat{\mathcal{B}}$, respectively. Since $\hat{\varphi}_1$ is sufficiently small for all values of ω (cf. Fig. 6), to estimate $\hat{\mathcal{F}}$ we may replace $\hat{\vartheta}$ by the function

$$\vartheta^s(\varphi) = \begin{cases} \hat{\vartheta}(0) & \text{for } 0 \leq \varphi \leq \hat{\varphi}_1 \\ 0 & \text{otherwise.} \end{cases} \tag{4.1}$$

This amounts to replace the crater of $\hat{\mathcal{B}}$ by another whose profile is an arc of logarithmic spiral. An easy computation shows that

$$\mathcal{F}_0 - \hat{\mathcal{F}} = 2\pi\rho_0^2 w_0 \sqrt{\omega}\, \hat{\varphi}_1^2 (g(\omega) - 1) + o(\hat{\varphi}_1^2) \tag{4.2}$$

where the function g is defined by

$$g(\omega) = \frac{\omega + 1}{2\sqrt{\omega}}. \tag{4.3}$$

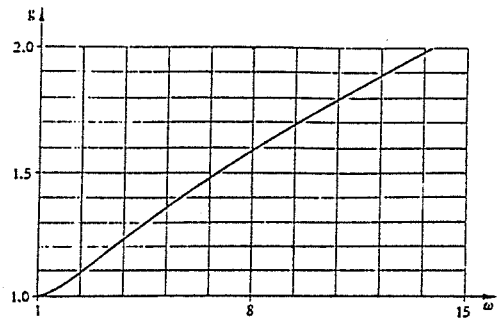

Fig. 7.

The graph of g is plotted in Figure 7. Since $g(\omega) > 1$ for all $\omega > 1$, we conclude that $\mathscr{F} < \mathscr{F}_0$. Thus $\hat{\mathscr{B}}$ is the stable shape of the drop when $\omega > 1$.

At first glance the crater of $\hat{\mathscr{B}}$ looks like a cone. Figures 8 and 9 illustrate such a shape for $\omega = 2$ and $\omega = 10$, respectively. The angle γ' is the semi-amplitude of the cone and the segment QP is its apothem.

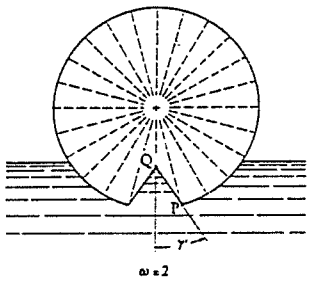

Fig. 8.

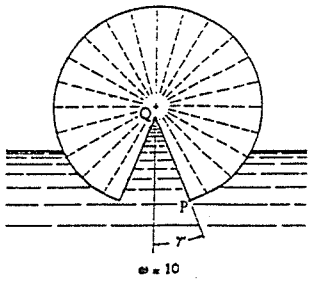

Fig. 9.

At a closer inspection, the crater of $\hat{\mathscr{B}}$ differs slightly from a cone, as is shown in Figure 10, where the scale unit of the vertical axis is sufficiently larger than that of the horizontal axis.

It follows from (3.12) that the angle γ'' is such that $\gamma' + \gamma'' = \arcsin 1/\sqrt{\omega}$.

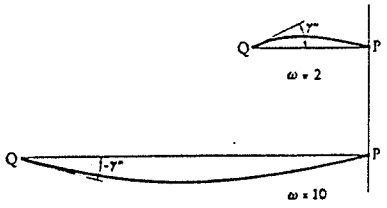

Fig. 10.

5 - Asymptotic stable shapes

In this section we study the solution of (3.6) that represents the stable shape $\hat{\mathscr{B}}$ when ω becomes very large. Our main purpose here is to check the consistency of the analysis carried out in the previous sections. If $\omega \gg 1$, equation (3.6) may be replaced by

$$t' = -\frac{1}{2\tau(1+\tau^2)}\left(4\tau t^2 + \frac{1}{\omega}t^3 - t\right) \tag{5.1}$$

in the strip $\tau \geq 0$, $-\omega \leq t \leq -\sqrt{\omega}$ (cf. eq. (3.8)). By use of the change of variables

$$s = \frac{1}{\omega} t \tag{5.2}$$

we give (1) the form

$$\frac{1}{\omega} s' = -\frac{1}{2\tau(1+\tau^2)} \left(4\tau s^2 + s^3 - \frac{1}{\omega} s\right) \tag{5.3}$$

in the strip $\tau \geq 0$, $-1 \leq s \leq -1/\sqrt{\omega}$. An easy computation shows that (3) may also be written as

$$\frac{s'}{\omega} = -\frac{s(s-s_1)(s-s_2)}{2\tau(1+\tau^2)} \tag{5.4}$$

where

$$s_1(\omega, t) = -2\tau + (4\tau^2 + \frac{1}{\omega})^{1/2} \qquad s_2(\omega, t) = -2\tau - (4\tau^2 + \frac{1}{\omega})^{1/2}. \tag{5.5}$$

Let $\delta_0 > 0$ and $\delta_1 > \delta_0$ be given. We denote by s_ω any negative and non-increasing solution to (4) of class C^1 in $[\delta_0, \delta_1]$. It follows from (4) that

$$s_2(\omega, \tau) < s_\omega(\tau) < 0 \quad \text{for all} \quad \delta_0 \leq \tau \leq \delta_1 \quad \text{and} \quad \omega > 1. \tag{5.6}$$

If s_ω is such that

$$\lim_{\omega \to \infty} \frac{1}{\omega} \max_{[\delta_0, \delta_1]} |s'_\omega| = 0 \tag{5.7}$$

then, by using (5.6) and taking the limit as $\omega \to \infty$ in (5.4), we arrive at

$$\lim_{\omega \to \infty} (s_\omega(\tau) - s_2(\omega, \tau)) = 0 \quad \text{for all} \quad \delta_0 \leq \tau \leq \delta_1. \tag{5.8}$$

Since s_2 approaches the function $s_2 = -4\tau$ when $\omega \to \infty$, we conclude from (5.8) that

$$\lim_{\omega \to \infty} s_\omega(\tau) = -4\tau \tag{5.9}$$

uniformly in all closed intervals of the positive real line. In particular, if (5.7)

holds,

$$\lim_{\omega\to\infty} s_\omega(\frac{1}{4}) = -1;$$

this proves that the line $\operatorname{tg}\hat{\varphi}_1 = \frac{1}{4}$ is an asymptote to the graph of Fig. 6.

We have indeed found numerical solutions s_ω of (5.4) that satisfy (5.7) and $s_\omega(0) = -1/\sqrt{\omega}$. One can see from Figure 11 how these solutions get close to the locus $s' = 0$ (whose equation is $s = s_2(\omega, \tau)$) when $\omega \to \infty$.

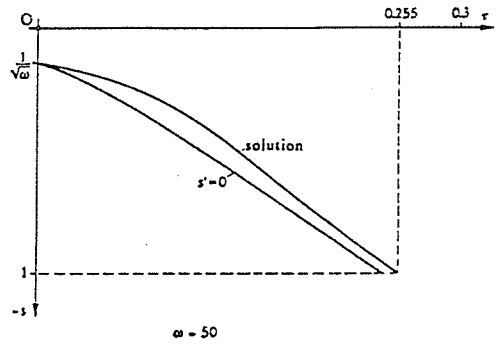

Fig. 11.

We finally note that, by (5.3), $s'_\omega(0) = -2$ whenever $s_\omega(0) = -1/\sqrt{\omega}$, for all $\omega > 1$. Thus the hypothesis that $\delta_0 > 0$ cannot be removed from the above analysis.

Conclusion

We predict an instability phenomenon for the shape of a drop of nematic liquid crystal floating on an isotropic liquid. For suitable values of the anchoring energy the stable shape bears a crater underneath the plane of buoyancy. This might provide a further way to explore the dependence of the anchoring energy on the temperature and the material. To our knowledge, however, experiments to this end have not yet been carried out.

References

[1] J. L. ERICKSEN, *Equilibrium theory of liquid crystals*, in *Advances in liquid crystals*, vol. II, G. H. Brown Ed., Academic Press, New York, 233-298, 1976.

[2] F. C. FRANK, *On the theory of liquid crystals*, Discussions Faraday Soc. **25** (1958), 19-28.

[3] I. HALLER, *Elastic constants of nematic crystalline phase for* MBBA, J. Chem. Phys. **57** (1972), 1400-1405.

[4] M. KLÉMAN, *Points, lines and walls*, J. Wiley and Sons, Chichester, 1983.

[5] D. LANGEVIN, *Analyse spectrale de la lumière diffusée par la surface libre d'un crystal liquide nématique. Measure de la tension superficielle et des coefficients de viscosité*, J. Phys. (Paris) **33** (1972), 249-256.

[6] S. NAEMURA: $[\bullet]_1$ *Measurement of anisotropic interfacial interactions between a nematic liquid crystal and various substrates*, Appl. Phys. Lett. **33** (1978), 1-3; $[\bullet]_2$ *Anisotropic interactions between* MBBA *and surface-treated substrates*, J. Phys. (Paris) **40** (1979), C-3, 514-518.

[7] C. W. OSEEN, *Probleme für die Theorie der anisotropen Flüssigkeiten*, Z. Kristallographie **79** (1933), 173-185.

[8] D. RIVIÉRE, J. LÉVY and C. GUYON, *Determination of anchoring energies from surface tilt angle measurements in a nematic liquid crystal*, J. Phys. (Paris) Lett. **40** (1979), L 215-218.

[9] T. J. SLUCKIN and A. PONIEWIERSKI, *Orientational wetting transitions and related phenomena in nematics*, in *Fluid interfacial phenomena*, C. A. Croxton Ed., J. Wiley and Sons, Chichester, 1986.

[10] E. G. VIRGA, *Drops of nematic liquid crystals*, Arch. Rational Mech. Anal. **107** (1989), 371-390.

Abstract

We predict the equilibrium shapes of a drop of nematic liquid crystal floating on a liquid. Under plausible assumptions, we reduce the free energy to a functional that depends on a dimensionless parameter ω related to the temperature. We find that when $-1<\omega\leq 1$ the only equilibrium shape of the drop is a ball. When $\omega>1$ there are two equilibrium shapes, namely a ball and a ball bearing a crater underneath the plane of bouyancy. The latter shape minimizes the free energy. The size of the crater depends on ω, and it vanishes when $\omega=1$. Thus a bifurcation with exchange of stability occurs at this point.

***